
SAR change detection based on Generalized Gamma distribution divergence and auto-threshold segmentation

GAO Cong-shan^{1 2}, ZHANG Hong^{1*}, WANG Chao¹

1. Center for Earth Observation and Digital Earth, CAS, Beijing, CHINA, 100086

2. Graduate University of Chinese Academy of Sciences, Beijing, CHINA, 100049

(serein_mars@163.com, hzhang@ceode.ac.cn, cwang@ceode.ac.cn)

Abstract

This paper first utilizes generalized Gamma model to fit the statistical characteristics of co-registered SAR images. Then, extract the difference map through measuring the similarity between PDFs by Kullback–Leibler Divergence. Afterwards, apply a combination of KS & KL test to evaluate and choose fitting function of the difference map for the model-based KI threshold segmentation automatically. Experiment was carried on the multi temporal SAR images for Beijing, acquired by TerraSAR and Radarsat-2, as well as Shunyi District of Beijing, acquired by Envisat-ASAR. Such results confirmed the proposed method is more sensitive in detecting regions that have no variance in mean value, but differ in texture, than traditional methods

Keywords: Kullback–Leibler Divergence, Generalized Gamma, KI, Change Detection

1. Introduction

Since the extensive application of SAR in change detection, scholars home and abroad carried out series of studies based on the specificity of SAR imaging mechanism, thus mainly focus on the steps for difference map extraction and threshold segmentation.

For difference map extraction, Rignot [1] proved the effectiveness of mean ratio detector (MRD) in 1993. Inglada [2] introduced the

concept of KL, as a quantitative measurement of PDFs' difference in 2003; Mercier [3] optimized the calculation of KL through edgeworth approximation in 2007. So far, only some classic model, such as Gaussian, Pearson, and Rayleigh, has been applied into the actual work.

All threshold segmentation methods are originated from three traditional categories [4]. Square Error Algorithm (Ostu, 1978), most efficient, but doesn't work when ratio of change and unchanged area is very small; Maximum Entropy Algorithm (Shannon, 1979), over dependent on prior knowledge, and vary with different choice of entropy criteria significantly; Minimum Error Method (Kittler & Illingworth, 1986), extension of Bayes minimum error probability, improved by G. Moser in 2006 [5], since its cost and criterion function varies with fitting model chosen.

In this paper, we combined generalized Gamma distribution to KL, which effectively quantified differences in statistical characteristic of multi-temporal SAR image, and then used a combination of KS and KL Test to select the best fitting function of difference map automatically, thus improving the traditional methods of threshold segmentation KI (Fig 1-1).

*This work is supported by funding form 863 program (Project No.2009AA12z118) and NSFC (Project No.

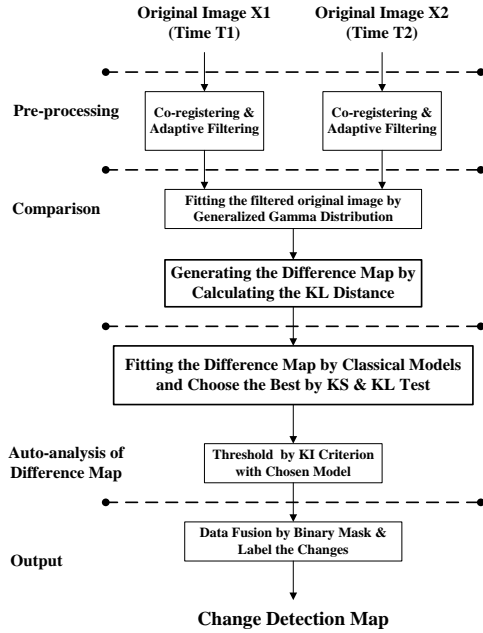


Fig 1-1 Flow Chart of Proposed Algorithm

2. Problem Formulation

2.1. Generalized Gamma Distribution

We proposed a 3-parameter generalized gamma distribution (1) to achieve the statistical modeling of SAR image.

$$f_{G\Gamma-pdf}(x; a, b, c) = \frac{c}{b\Gamma(a)} \left(\frac{x}{b}\right)^{ac-1} \exp\left[-\left(\frac{x}{b}\right)^c\right] \quad (1)$$

Where, a is shape parameter; b is scale parameter; c is power parameter.

Fig 2-1 shows several modes of generalized gamma which is extremely close to typical models. Thus means generalized gamma not only owns an accurate description of heavy-tail, but also fits each sub-region with different models by estimated parameters.

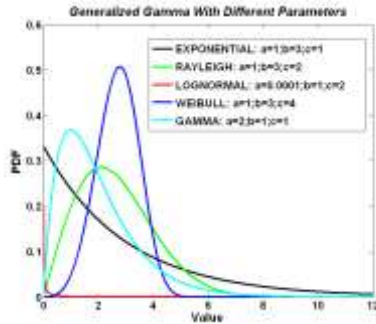


Fig 2-1 Classical Fitting Modes of Generalized Gamma

2.2. Kullback-Leibler (KL) Distance

Use KL divergence to measure degree of regional statistics similarity between subsets (2).

$$K(Y|X) = \int \log \frac{f_x(x)}{f_y(x)} f_x(x) dx \quad (2)$$

Here, $f_x(x)$ and $f_y(x)$ were the generalized gamma model for corresponding pixel neighborhood in T1 and T2 image with the estimated parameters by moment [6]. To address the asymmetry in KL, Jensen-Shannon Divergence (3) by Jeffrey (2000) was taken.

$$f_Q(x) = (f_x(x) + f_y(x))/2 \quad (3)$$

$$KLDIV = (K(Y|Q) + K(X|Q))/2$$

2.3. Auto-KI Threshold Segmentation

An adaptive KI threshold segmentation (4) was proposed to extract a binary mask of change regions.

$$\hat{P}_{ir} = \sum_{z \in R_{ir}} h(z)$$

$$c(z, \tau) = \begin{cases} -\ln \hat{P}_{0r} - \ln p_0(z | \hat{m}_{0r}, \hat{\sigma}_{0r}), & z < \tau + 1; \\ -\ln \hat{P}_{1r} - \ln p_1(z | \hat{m}_{1r}, \hat{\sigma}_{1r}), & \tau < z < Z \end{cases} \quad (4)$$

$$J(\tau) = \sum_{z=0}^{Z-1} h(z)c(z, \tau)$$

$$T = \arg \min \{J(\tau) : \tau=0, 1, 2, \dots, Z-1\}$$

$J(\tau)$ is criterion function; $c(z, \tau)$ is cost function; $h(z)$ is probability density histogram.

Calculate posteriori probability of ω_1 and ω_0 by corresponding prior and likelihood probability.

As difference map captured from different fitting models or origin image, may agree with different distributions, a combination of KS & KL test was applied to select the best fitting function automatically. Moreover, generalized Gauss, G0, and Joint Lognormal & Rayleigh were introduced to fit the difference map better.

3. Experimental Results

3.1. Experimental Dataset

Table 1 is multi-temporal SAR image for Beijing (Fig 3-1), and Shunyi District of Beijing (Fig 3-2).

Table 1 Experiment Dataset

Area	Beijing	Beijing	Shunyi	Shunyi
acquisition Time	20080304	20081022	20040601	20050517
Sensor	TerraSAR	RADARSAT-2	ASAR	ASAR
Polarization	VV	VV	HH	HH
Resolution (m)	5.6×8	5.6×8	30×30	30×30
Image Size (Pixels)	1770×1995	1770×1995	1024×1024	1024×1024

(* All neighborhood window size selected as 13*13)

3.2. Difference Map Extraction

Both MRD and Generalized gamma KL methods had been applied to the TerraSAR-X and Radarsat-2 image of Beijing on March and October in 2008. According to the theory proposed by F.T. Ulaby [7], amount of false alarm may appear by MRD method, since it is not sensitive to the phenomenon mean value of the window remains, while the texture changes.

In order to verify the superiority of KL difference map extraction with generalized gamma, we selected three corresponding sample area (Fig 3-3) for experiments. A is the Garden of Perfection and Brightness; B and C are two parts of Olympic Forest Park Wetland. The total size of sample area is 1164048 pixels, actual change pixel is 132608, and unchanged pixel is 1031440. Do statistics for detection rate and false alarm rate of both the proposed and MRD method based on different thresholds, draw Receiver Operating Characteristics (ROC).



Fig 3-3 Sample District Selection in Original Image

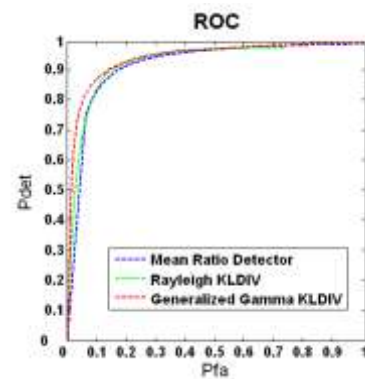


Fig 3-4 ROC Curve for Different Detectors

For ROC, the greater area below curve is, the better effect detection method achieves [8]. As showed in Fig 3-4, the effect of the proposed KL detector based on generalized Gamma (Red) is significantly superior to the traditional MRD (Blue) difference map extraction method. Moreover, the KL detector based on Rayleigh (Green) is just located between the two.

3.3. Threshold Segmentation

This paper achieve the selection of the best fitting model by calling the KL test proposed in section 2.2, to compare the best fitting model selected through KS test, as well as the model of generalized Gauss.

Table 2 KS Test Results for Different Fitting Model

Kolmogorov	Shunyi	Beijing	Beijing
-Smimov	GGamma	GGamma	Rayleigh
(KS)	KLDIV	KLDIV	KLDIV

LOGNORMAL	0.04593	0.05962	0.06671
GAMMA	0.10155	0.02070	0.08612
RAYLEIGH	0.47975	0.10716	0.46306
WEIBULL	0.08565	0.05034	0.08876
K	0.14910	0.04105	0.10292
MIX (RAY&LN)	0.02193	0.02737	0.06536
G0	0.07289	0.03665	0.38563

Table 3 KL Test Results for Best Fitting Model and Generalized Gauss Model

Jensen- Shannon (KL)	Shunyi GGamma KLDIV	Beijing GGamma KLDIV	Beijing Rayleigh KLDIV
Gamma	0.0828	0.0473	0.1630
G-Gauss	0.1900	0.2086	0.1704
MIX (RAY&LN)	0.0473	0.0561	0.0271

For the KL difference map of Shunyi with Generalized Gamma, the Rayleigh & Lognormal joint distribution fits best; for the KL difference map of Beijing with Generalized Gamma, the Gamma distribution fits best; for the KL difference map of Beijing with Rayleigh, also the Rayleigh & Lognormal joint distribution fits best. Such confirms that both the selection of different features and different fitting distribution for SAR image may influence the distribution of KL difference map (Table 2 and 3). Accordingly, Gamma model was selected for KI threshold segmentation in this experiment (Fig 3-6).

3.4. Methods Evaluation

Compare the proposed method with the most popular MRD & KI threshold segmentation with generalized gauss by Lorenzo (Fig 3-5), based on Fig 3-1. According to on-site survey, the main changes should be the construction of the Music Station and the perfusion of water to the artificial wetlands in Olympic Forest Park in 2008, as well as the erosion of the Algae on the surface of the

water in the Garden of Perfection and Brightness by the Algae Worm.



Fig 3-5 G-Gauss Threshold for MRD Difference Map (a) TerraSAR 20080304 (b) Radarsat-2 20081022

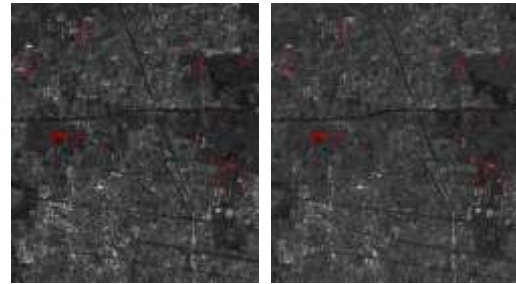


Fig 3-6 Gamma Threshold for G-Gamma KL Map (a) TerraSAR 20080304 (b) Radarsat-2 20081022

However, experimental results show that, KI threshold segmentation with generalized gauss is an effective method to avoid false alarm caused by corrugated surface in MRD progress; but for changes taken place in small regions, it was not sensitive enough. The proposed method has effectively solved this problem, and detected the significant changed area in artificial wetlands of Olympic Forest Park that was missed by generalized Gauss KI Algorithm.

4. Discussion and Conclusions

The proposed method extracted difference map by KL with generalized gamma to obtain the radiation value and texture information, then realized adaptive KI threshold segmentation by a combination of KS and KL test. Compared with traditional change detection methods, this approach overcomes the problem of information loss in local texture characteristics effectively, especially for those changes in farmland species, wetlands, and other small region. The further

optimization and efficiency of this method will be the focus of the study in the next step.

References

- [1] E. Rignot et al., "Change Detection Techniques for ERS-1 SAR Data", *IEEE Transactions on Geoscience and Remote Sensing*, 1993, 31(4), pp.896-906
- [2] J. Inglada et al., "Change detection on SAR images by using a parametric estimation of the Kullback-Leibler divergence", *Proc. IGARSS, Toulouse, France*, 2003, pp.4104–4106.
- [3] G Mercier and S Derrode, "SAR image change detection using distance between distributions of classes", *IEEE Transactions on Geoscience and Remote Sensing*, 2004, 74(4), pp.3872-3875
- [4] J. Kittler and J. Illingworth, 1986, Minimum Error Thresholding[J]. *Pattern Recognition.*, 19, 41–47
- [5] G Moser et al. "Generalized Minimum-Error Thresholding for Unsupervised Change Detection from SAR Amplitude Imagery". *IEEE Transactions on Geoscience and Remote Sensing*, 2006, pp.614-619
- [6] C. Gomes and A. Combes, "Parameter estimation of the generalized gamma distribution", *Mathematics and Computers in Simulation*, 2008, pp.955–963
- [7] F. T. Ulaby et al., 1986, Textural information in SAR images, *IEEE Trans. Geosci. Remote Sens.*, GRS-24, 235–245.
- [8] Huo Chun-lei et al., 2008.3, Object-level Change Detection Based on Multiscale Fusion [J], *Acta Automatica Sinica*, 34(3), 251-257